Cell

Article

# Spatial Map of Human T Cell Compartmentalization and Maintenance over Decades of Life

Joseph J.C. Thome,[1,3,6] Naomi Yudanin,[1,3,6] Yoshiaki Ohmura,[2] Masaru Kubota,[2] Boris Grinshpun,[4] Taheri Sathaliyawala,[1,7] Tomoaki Kato,[2] Harvey Lerner,[5] Yufeng Shen,[4] and Donna L. Farber[1,2,3,*]

[1]Columbia Center for Translational Immunology, Columbia University Medical Center, New York, NY 10032, USA
[2]Department of Surgery, Columbia University Medical Center, New York, NY 10032, USA
[3]Department of Microbiology and Immunology, Columbia University Medical Center, New York, NY 10032, USA
[4]Department of Systems Biology and Biomedical Informatics, and the JP Sulzberger Columbia Genome Center, Columbia University, New York, NY 10032, USA
[5]The New York Organ Donor Network (NYODN), New York, NY 10001, USA
[6]Co-first authors
[7]Present address: Merck Research Labs, Palo Alto, CA 94304
*Correspondence: df2396@cumc.columbia.edu
http://dx.doi.org/10.1016/j.cell.2014.10.026

## SUMMARY

Mechanisms for human memory T cell differentiation and maintenance have largely been inferred from studies of peripheral blood, though the majority of T cells are found in lymphoid and mucosal sites. We present here a multidimensional, quantitative analysis of human T cell compartmentalization and maintenance over six decades of life in blood, lymphoid, and mucosal tissues obtained from 56 individual organ donors. Our results reveal that the distribution and tissue residence of naive, central, and effector memory, and terminal effector subsets is contingent on both their differentiation state and tissue localization. Moreover, T cell homeostasis driven by cytokine or TCR-mediated signals is different in CD4+ or CD8+ T cell lineages, varies with their differentiation stage and tissue localization, and cannot be inferred from blood. Our data provide an unprecedented spatial and temporal map of human T cell compartmentalization and maintenance, supporting distinct pathways for human T cell fate determination and homeostasis.

## INTRODUCTION

T lymphocytes, a critical component of the adaptive immune system, provide lifelong protection against pathogens by orchestrating immune responses at diverse sites of infection. Naive T cells emerge from the thymus and populate lymphoid tissues sites, where they differentiate to effector T cells upon antigen encounter, and subsequently can develop into long-lived memory T cells. The complement of T cells within an individual is heterogeneous, consisting of naive T cells, short-lived or terminally differentiated effector cells (also designated as TEMRA), and memory T cells that accumulate with successive antigen encounters and are the predominant T cell subset in adults (Farber et al., 2014; Saule et al., 2006). Memory T cells are comprised of multiple subsets defined by their migration capacities and tissue residence, including central (TCM) memory cells in circulation and lymphoid sites, effector memory (TEM) cells circulating through blood and peripheral sites (Sallusto et al., 2004), and a recently identified resident memory T cell (TRM) subset retained in tissues such as lungs, intestines, skin, liver, and genital mucosa (Clark et al., 2006; Mueller et al., 2013; Purwar et al., 2011; Sathaliyawala et al., 2013; Turner et al., 2014a). Each of these subsets has specific roles in preserving immunity: maintenance of naive T cells is important for responses to new antigens, and memory T cells mediate protection to diverse pathogens encountered at multiple anatomic locations. Identifying the pathways for memory generation and maintenance is therefore critical for designing effective ways to promote lifelong T-cell-mediated immunity in humans, for which no strategies currently exist.

The development and maintenance of T cell subsets in humans remain poorly understood for several reasons. Primarily, most studies of human T cells are confined to sampling of peripheral blood, which contains less than 3% of the total T cells in the body (Ganusov and De Boer, 2007). There are few studies analyzing T cells in lymphoid tissue, where most immune responses are initiated, and only isolated studies in mucosal sites, where effector and memory T cells function and are maintained (Farber et al., 2014). This limited sampling in humans makes it virtually impossible to follow an immune response in vivo as in animal models, thus we lack essential insights into human T cell lineage and maintenance. Moreover, humans enjoy a long lifespan, with potential for dynamic changes in the T cell compartment due to increased antigen experience, decreased thymic output, and alterations in T cell homeostasis. However, most studies of human T cells examine cohorts of limited age

range, while studies of aging and T cells compare young and aged cohorts in discrete, nonoverlapping groups, rather than assessing how T cell subset composition may dynamically alter over the course of a lifetime. Defining the fundamental properties of human T cell subsets throughout the body can therefore provide an understanding of their lineage relationships and differentiation pathways in ways not previously possible.

Through an ongoing collaboration and research protocol with the New York Organ Donor Network (NYODN), we are studying human immunity by investigating immune cell subsets in multiple tissue sites obtained from individual organ donors. We previously demonstrated that obtaining blood, lymphoid, and mucosal tissues during the time of organ acquisition for life-saving transplantation enables analysis of functional lymphocytes in situ (Sathaliyawala et al., 2013). Importantly, these initial studies revealed the potential to use this tissue resource as a "human model system" to address previously unanswerable questions in human T cell biology about differentiation and lifelong maintenance.

Here, we present a quantitative system-wide analysis of T cell differentiation, homeostasis and persistence in blood, lymphoid, and mucosal tissues obtained from a highly diverse cohort of 56 organ donors aged 3–73 years. We incorporate an analysis of naive, memory, and effector T cells with functional markers of homeostasis, activation, and tissue residence along with quantification of in situ turnover and TCR clonal distribution to reveal distinct patterns of compartmentalization, maintenance and proliferation of human T cells. Notably, we show that mucosal sites are predominantly populated with TEM cells that bear features of TRM cells, which are discretely compartmentalized and stably maintained over life in mucosal tissues, while subsets in lymphoid sites undergo age-associated changes. Circulating naive T cells decrease in lymphoid sites with a corresponding increase in TEM and TEMRA, while TCM cells persist at a steady frequency in circulation and tissues throughout life with a significant fraction continuously turning over. We identify key differences in memory $CD4^+$ and $CD8^+$ T cell homeostasis among lymphoid and mucosal tissues, with memory $CD4^+$ T cell subsets responding to cytokine-mediated signals, and memory $CD8^+$ T cells exhibiting cytokine-driven responses in lymphoid tissue and cognate signals in mucosal sites. Moreover, TCR sequencing of TEM cells in different sites revealed increased circulation and clonality of $CD8^+$ TEM, while $CD4^+$ TEM are primarily resting and compartmentalized. Our results reveal localization-dependent heterogeneity in T cell maintenance and homeostasis, implicating distinct pathways for peripheral differentiation of $CD4^+$ and $CD8^+$ T cell subsets.

## RESULTS

### Tissue Compartmentalization of Human T Cell Subsets Is Conserved among Diverse Individuals

We have established a unique human tissue resource through a collaboration and research protocol with the NYODN, in which multiple lymphoid and mucosal tissues are obtained from research-consented human organ donors (Sathaliyawala et al., 2013). Here, we acquired tissues from donors across all ages of life for a unique assessment of human immune cell compartmentalization and maintenance. The 56 individuals used for this study are highly diverse, ranging in age from 3–73 yr (median age 37.5, Figure 1A), and representing all major races/ethnicities (white, 43%; hispanic, 32%; black, 23%; and Asian, 2%; Figure 1B) and body types (Table S1 available online). All donors were healthy ($HIV^-$, $HBV/HCV^-$, cancer-free, free of systemic infections) prior to brain death due to noninfectious traumas such as cerebrovascular stroke (37%), head trauma (23%), anoxia (36%), or other causes (4%) (Figure 1C and Table S1). The tissues analyzed from each donor sample circulation, lymphoid, and mucosal sites and include peripheral blood, spleen, inguinal lymph node (ILN, draining the peripheral skin and muscle), lung-draining lymph node (LLN), lungs, mesenteric lymph node (MLN, draining the intestines), small intestine (jejunum and ileum), and colon.

We obtained viable lymphocyte populations from blood and eight different lymphoid and mucosal tissue sites (see Experimental Procedures) that enabled unprecedented spatial and temporal phenotypic, functional and molecular analysis (Figure 1D). The composition of $CD4^+$ and $CD8^+$ T cell subsets (naive, TCM, TEM, and TEMRA) was assessed in nine anatomic sites, and the resultant 72 populations were analyzed for the expression of functional markers of tissue residence, longevity, and turnover. We further investigated memory T cell maintenance and compartmentalization on the clonal level using TCR deep sequencing to quantify $CD4^+$ and $CD8^+$ T cell clonal distribution among multiple lymphoid sites (Figure 1D). We statistically analyzed all these parameters to quantify age- and tissue- associated changes (see Extended Experimental Procedures). These multifaceted analyses enabled an assessment of human T cell differentiation and maintenance in the body over life. Donors used for each aspect of this study are indicated in Table S2.

We assessed T cell subset composition in each tissue and variance among tissues and donors by flow cytometric analysis of well-established markers. $CD3^+CD19^-CD4^+$ and $CD8^+$ T cell subsets were further defined by coordinate expression of the CD45RA and chemokine receptor type 7 (CCR7), delineating naive ($CD45RA^+/CCR7^+$), TCM ($CD45RA^-/CCR7^+$), TEM ($CD45RA^-/CCR^-$), and TEMRA cells ($CD45RA^+/CCR7^-$) (Figure 2A). A representative staining profile of CD45RA and CCR7 expression by $CD4^+$ and $CD8^+$ T cells (Figure S1) and compiled results from 39 donors (Figure 2B) reveals a distinct pattern of subset composition in circulation (blood and spleen), lymph nodes, and mucosal tissues, that differs between $CD4^+$ and $CD8^+$ T cells. Both $CD4^+$ and $CD8^+$ T cells exhibited a similar distribution of TEM and naive subsets, with TEM predominating in mucosal tissues and naive cells only significantly present in blood and lymphoid tissues. However, the frequency and tissue localization of TCM and TEMRA cells differed between $CD4^+$ and $CD8^+$ T populations, with TCM cells more prevalent among $CD4^+$ T cells, comprising 20%–30% of total CD4 T cells in blood, lymph nodes, and lungs, compared to < 10% of $CD8^+$ T cells in these sites (Figure 2B). Conversely, TEMRA cells were predominantly $CD8^+$, and localized primarily to blood, spleen, and lung, with low frequencies (<10%) in lymphoid and mucosal tissues (Figure 2B, right). Remarkably, these tissue- and $CD4^+/CD8^+$-specific T cell subset distribution patterns were highly conserved among diverse individuals, as evidenced by the low

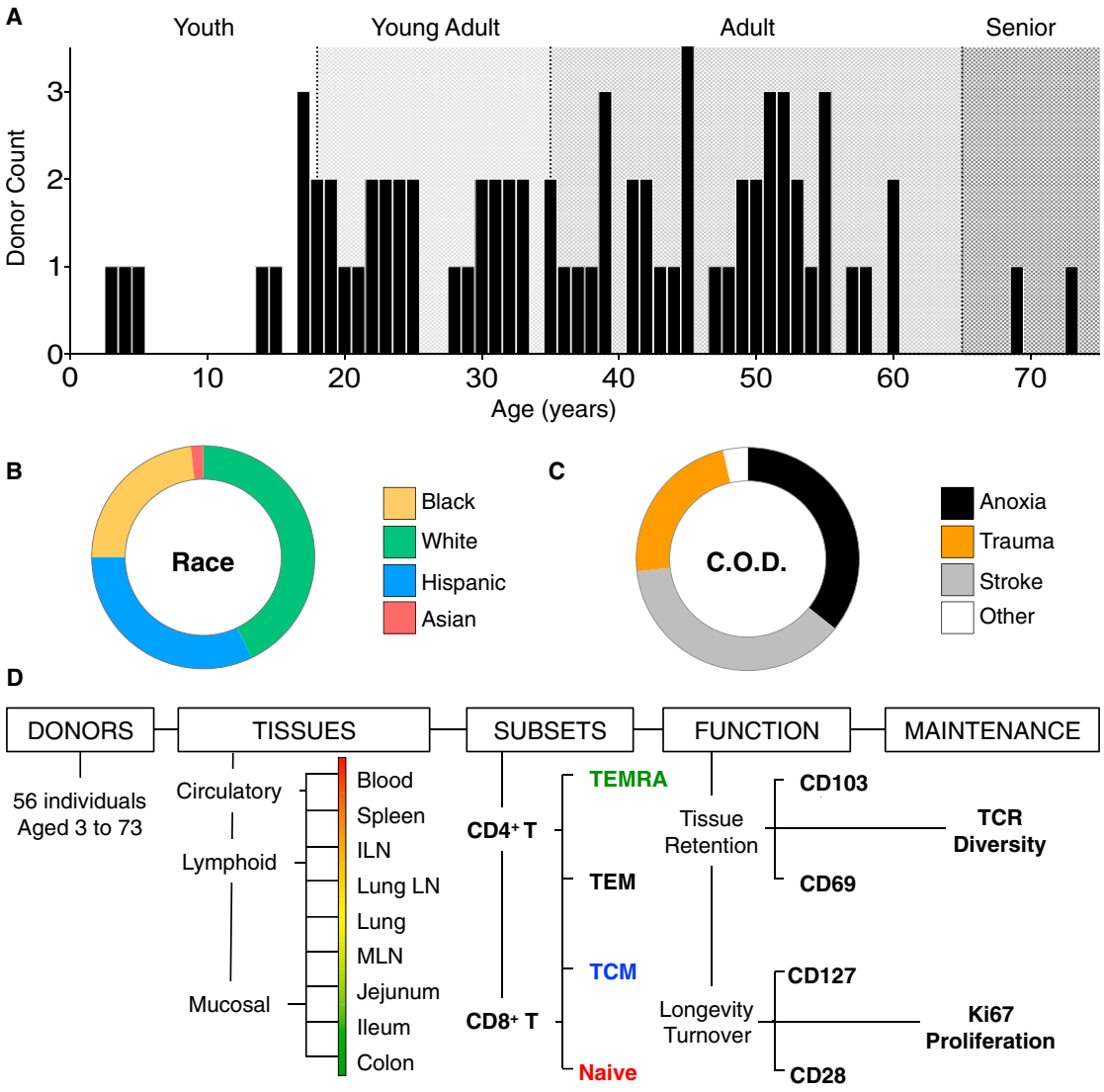


**Figure 1. Characteristics of the Human Donor Population and Analysis Overview**

Lymphocyte frequency, distribution, function and maintenance was assessed in 9 tissue sites acquired from 56 deceased organ donors, aged 3–73. (A) Age distribution of analyzed donors grouped into four life stages: Youth (0–5 years, white), Young Adult (16–35 years, light gray), Adult (36–65 years, gray), and Senior (66+ years, dark gray). (B) Race distribution of the organ donor population: White (green), Hispanic (blue), Black (yellow), and Asian (red). (C) Cause of death distribution of the organ donor population: Cerebrovascular stroke (gray), Head Trauma (orange), Anoxia (black), other causes (white). Characteristics of each individual donor including age, gender, height, weight, cause of death and serology are detailed in Table S1. (D) Flow chart of different parameters investigated and the analyses performed for this study from 56 donors, with blood and 8 tissues from each donor, analyzing 8 distinct $CD4^+$ and $CD8^+$ T cell subsets in terms of their function, proliferation, TCR diversity and homeostasis.

variance in individual subset frequency at each site (Figure 2B and Table S3).

To analyze differential T cell subset compartmentalization among blood, lymphoid, and mucosal sites, we quantified the mean subset frequency variance in each tissue (see Experimental Procedures) (Figure 2C and Table S4). Overall, the distribution of $CD4^+$ and $CD8^+$ naive and TEM cells and $CD8^+$ TEMRA cells varied significantly among blood, lymphoid, and mucosal sites, while the frequency of TCM cells did not (Figure 2C). The distribution variance of $CD4^+$ and $CD8^+$ naive and TEM cells is low between circulation and lymphoid sites, yet increases significantly between circulation/lymphoid and mucosal sites (Figure 2C). Moreover, the distribution variance of $CD8^+$TEMRA is significant only in blood, spleen, and lung compared to mucosal and lymphoid tissue. Together, these results demonstrate that naive, TEM and $CD8^+$TEMRA cells are compartmentalized in distinct patterns in circulation, lymphoid, and mucosal tissues, which are consistent among diverse individuals. By contrast, TCM cells are not compartmentalized among tissues or individuals, suggesting either that they circulate among all sites, and/or

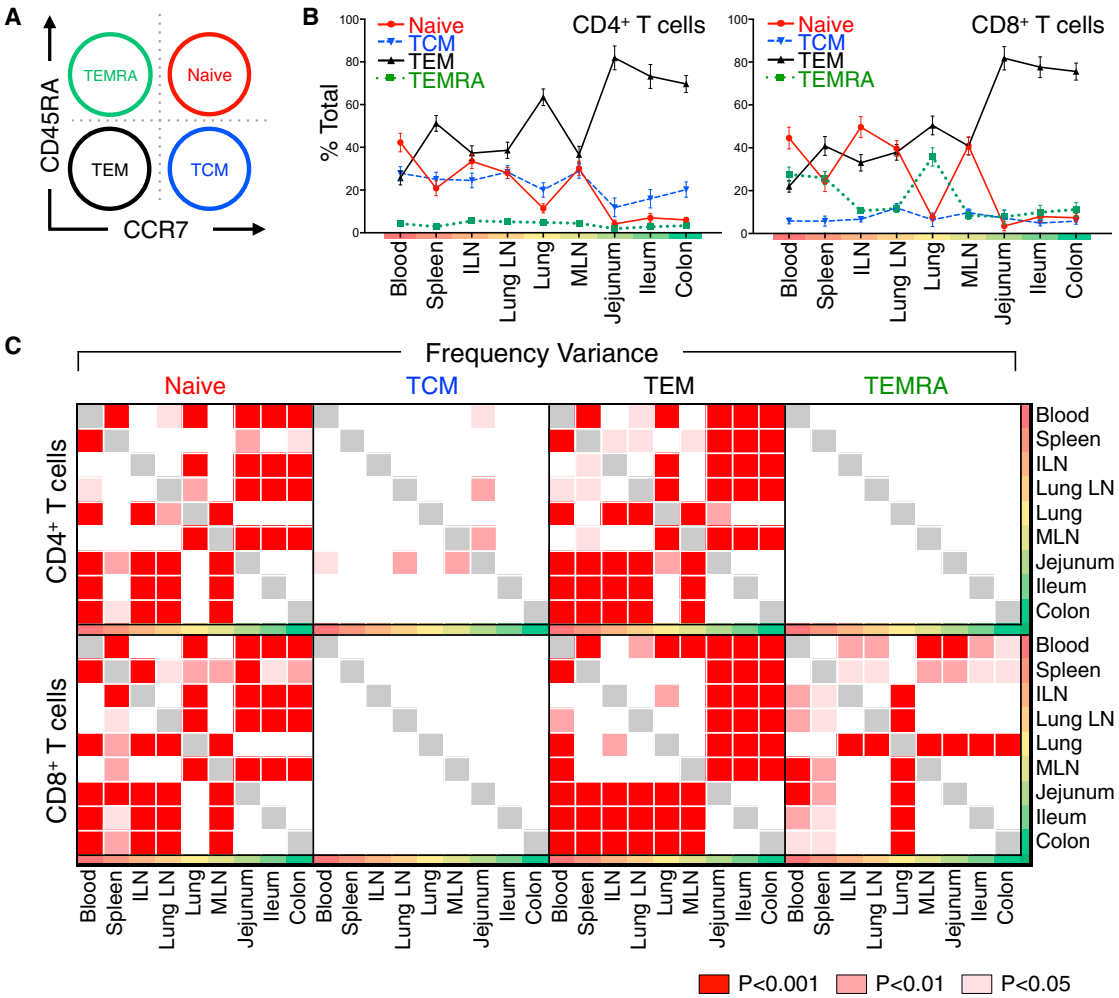


**Figure 2. Tissue Distribution of Naive, Memory, and Terminal Effector Subsets Remains Consistent between Diverse Donors**

Frequency of lymphocytes in 9 tissue sites isolated from organ donors was quantified by flow cytometry. (A) Gating strategy used to identify T cell subsets ($CD3^+$ $CD19^-CD4^+$ or $CD3^+$ $CD19^-CD8^+$ cells) based on CD45RA and CCR7 expression defining: $CD45RA^+/CCR7^+$ (Naive, red), $CD45RA^-/CCR7^+$ ("Central Memory" or TCM, blue), $CD45RA^-/CCR7^-$ ("effector-memory," TEM, black), and $CD45RA^+/CCR7^-$ ("Terminal effector" or TEMRA, green). Colors and abbreviations are used consistently throughout. (B) Mean frequency (±SEM) of each subset expressed as a percent of total $CD4^+$ (left) and $CD8^+$ (right) T cells in circulation, spleen, lymphoid tissue and mucosal sites (ordered from blood, red; to mucosal sites, green). Individual means and additional descriptive statistics are listed in Table S3. (C) Distribution variance between $CD4^+$ and $CD8^+$ T cell subset frequencies in 31 donors (Table S2) was assessed for each tissue by two-way ANOVA and adjusted for multiple comparisons by a Holm-Sidak correction. Significant frequency variances between tissue pairs are expressed as p values with red- and pink-shaded boxes indicating significant differences ($p < 0.001$, red; $p < 0.01$, light red; $p < 0.05$, pink) and white boxes indicating no significant difference in subset frequency between anatomic sites. Individual p values are listed in Table S4.

represent an intermediate population in T cell differentiation that is maintained through continuous turnover.

## Age Dependence of T Cell Subset Distribution in Lymphoid, but Not Mucosal, Sites

By analyzing donors of ages that span the majority of the human lifespan over six decades, we were able to assess whether T cell subset tissue distribution changes as a function of age. We plotted the relationship between age and subset distribution as a heat map of individual subset frequencies among blood and 8 tissue sites ordered by increasing age to generate a spatial and temporal atlas of human T cell subset composition (Figure 3A). The differential compartmentalization of naive, TEM and TEMRA subsets is conserved between individuals, with TEM subsets predominating in the mucosa, naive T cells localized to blood and lymphoid tissue, and $CD8^+$ TEMRA predominant in blood, spleen and lung independent of donor age. (Figure 3A). The low frequency of $CD4^+$ TEMRA and $CD8^+$ TCM subsets is also conserved in all individuals of all ages (Figure 3A).

To quantitatively probe the age dependence of subset distribution, we calculated the correlation between the subset frequencies in each tissue as a function of donor age. Our analyses revealed significant age-dependent changes in distribution of

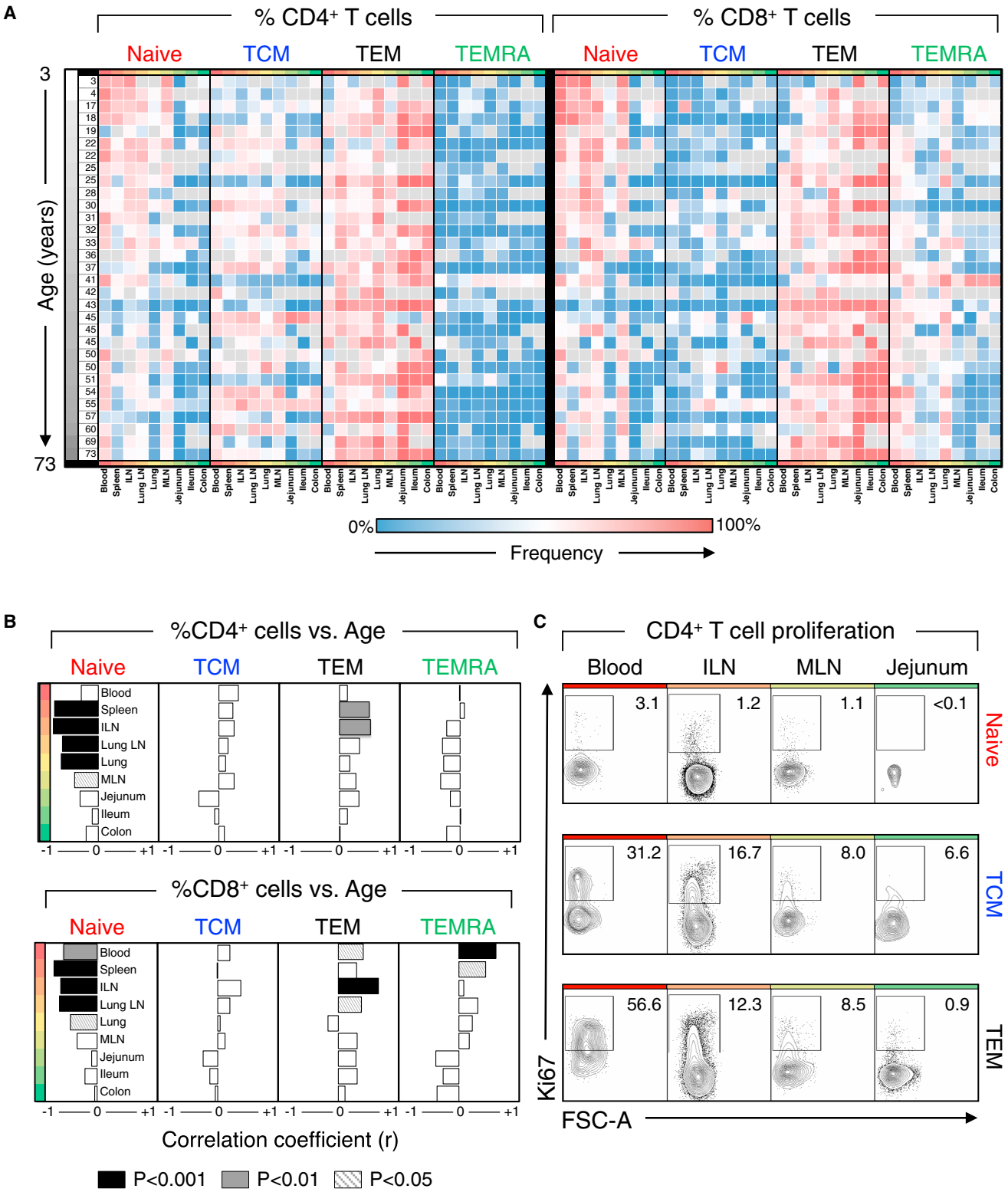


**Figure 3. Temporal Dependence of T Cell Distribution Varies by Subset and Compartment**

Lymphocyte frequency was quantified in 9 tissues from donors aged 3 to 73. (A) Heatmap of $CD4^+$ and $CD8^+$ T cell subset frequency (ranging from 0% (blue) to 100%, (red)) in individual donors from youngest (white) to oldest (black), from blood to lymphoid to mucosal sites. (B) Spearman correlation analysis of changes in

*(legend continued on next page)*

naive, TEM, and TEMRA subsets in blood and lymphoid tissue while their composition in mucosal tissue remain unchanged (Figure 3B). $CD4^+$ and $CD8^+$ naive T cell frequency decreased in lymphoid tissues with increasing age, though only the proportion of naive $CD8^+$ T cells decreased significantly in blood (Figure 3B, right). This depletion of naive T cells corresponded with a compensatory increase in lymphoid $CD4^+$ TEM in spleen and lymph nodes, $CD8^+$TEM in blood and lymph nodes, and $CD8^+$ TEMRA in blood and spleen (Figure 3B). The TCM subset (i.e., CD4 TCM), did not exhibit significant age-associated changes in any of the tissues (Figure 3B). These results demonstrate that age-associated changes in T cell composition only occurred with certain subsets and in specific sites, with lymph nodes undergoing dynamic changes and mucosal sites remaining stable.

The change in specific subset frequency could be due to either antigen-activation and/or homeostatic turnover. We investigated the contribution of ongoing homeostatic turnover to alterations in subset composition by examining Ki67 expression, upregulated by cycling cells. In blood, lymph nodes, and mucosal tissue of a representative donor, differences in Ki67 expression were observed between subsets and tissues: TCM and TEM had a higher proportion of $Ki67^+$ cells compared to naive T cells in all sites. Among $CD4^+$ memory subsets, the highest frequency of $Ki67^+$ cells was found in blood (30%–56%) followed by lymph nodes (8%–17%) with few $Ki67^+$ cells in mucosal sites (1%–7%) (Figure 3C). Though the overall percentage of $Ki67^+$ cells varied between donors, TCM and TEM subsets consistently had a higher proportion of cycling cells compared to naive T cells, particulatly among blood TEM cells (Figure S2A). Together, these results indicate that TEM and TCM subsets in lymphoid tissues and blood are dynamically altered throughout life, likely due to their continuous homeostatic turnover, while TEM cells in mucosal sites remains consistent over life with lower levels of in situ turnover. Loss of naive T cells, by contrast, is not associated with turnover, but with conversion to TEM/TEMRA cells, likely through antigen-mediated activation.

## Markers of Tissue Residence Are Predominant among TEM Cells in Tissues throughout Life

To assess the residence and tissue retention properties of different T cell subsets in each site, we examined tissue-, subset- and age-dependent expression of CD69, an early activation marker for T cells, recently established as a marker for TRM due to its constitutive expression by mucosal and skin TRM in mice and humans (Farber et al., 2014; Mueller et al., 2013; Sathaliyawala et al., 2013). Our analysis from blood and tissues of 29 donors reveals that CD69 expression is predominant among TEM in tissues, is established early, and remains stably maintained through life (Figure 4). T cell subsets in tissues are predominantly $CD69^-$, while in tissues CD69 expression is stratified among different subsets with 60%–90% TEM, 30%–60% TCM and TEMRA, and < 25% of naive T cells expressing CD69, consistent between diverse individuals (Figure 4B). Moreover, the highest frequency of $CD69^+$ TEM cells is observed in mucosal sites, with lower frequencies in lymphoid tissue (Figure 4B). Variance analyses reveal significant differences in CD69 expression by TCM, TEM, and TEMRA subsets between blood and tissues (Figure 4C). Correlation analysis reveals no significant change in CD69 expression by memory subsets in specific sites (Figure 4D). CD69 expression by T cells in tissues thus appears primarily dependent on differentiation, with TEM having the highest propensity for CD69 expression that is enhanced in mucosal sites.

As CD69 expression can also connote activation, we examined expression of the $\alpha_E$ integrin CD103, another key marker for $CD8^+$ TRM cells (Mueller et al., 2013; Turner et al., 2014a) also known to promote T cell retention in mucosal sites in mice (Schön et al., 1999; Strauch et al., 2001). As shown in representative flow cytometry plots (Figure 4E) and data compiled from multiple donors (Figure 4F), CD103 is coexpressed by $CD69^+$ $CD8^+$ TEM in mucosal tissues (lung, intestines) and intestinal-draining MLN (Figure 4E), indicating a canonical TRM phenotype. In peripheral lymphoid sites, including spleen, ILN, and LLN, there is minimal expression of CD103 by $CD69^+$ $CD8^+$ TEM, raising the question of whether $CD8^+$ TEM in lymphoid sites are resident or migratory. Because mouse and human memory CD4 T cells do not appreciably express CD103 (Sathaliyawala et al., 2013; Turner et al., 2014a), the migration and residence of lymphoid $CD69^+$ $CD4^+$ TEM, which undergo turnover and alterations with age, requires further investigation (see below).

## Coordinate Expression of CD28 and CD127 Identifies Tissue- and Subset-Specific T Cell Homeostasis

To assess potential mechanisms for the distinct dynamics of memory T cells in lymphoid and mucosal sites, we analyzed functional markers of activation/homeostasis including the costimulatory receptor CD28 and the homeostatic cytokine IL-7 receptor CD127 (IL-7R). CD28 expression is downregulated by human T cells in response to TCR-mediated activation, proliferation and replicative senescence (Lo et al., 2011; Vallejo et al., 1999), while IL-7R expression is downregulated following responses to IL-7 (Mazzucchelli and Durum, 2007) and by activated effector T cells (Kiazyk and Fowke, 2008). When examined separately, CD28 and CD127 expression by CD4 and CD8 T cell subsets in blood and tissues is variably expressed by TEM (and CD8 TEMRA subset) in mucosal sites (Figure S3). Coordinate expression of CD28/CD127 delineated four subsets (Figure 5A): $CD28^+CD127^+$, resting or unstimulated; $CD28^+CD127^-$, receiving IL-7 signals; $CD28^-CD127^+$, indicative of previous TCR-driven responses; and $CD28^-CD127^-$, a phenotype of antigen-activated effector cells. While naive and TCM subsets exhibited a predominant resting $CD28^+/CD127^+$ phenotype, CD28/CD127 expression by TEM cells (and $CD8^+$ TEMRA cells) varied between $CD4^+$ and $CD8^+$ T cells and lymphoid versus

lymphocyte tissue distribution with increasing age shows temporal changes in subset distribution in circulating and lymphoid sites. Correlation strength and directionality (r = −1, left to r = +1, right) is shown for each tissue ordered from blood to lymphoid to mucosal tissues. Correlation significance for each tissue is denoted by shading ($p < 0.05$, striped; $p < 0.01$, gray; $p < 0.001$, black). Individual r and p values are listed in Table S5.) (C) Ex vivo analysis of proliferation of naive, TCM, and TEM CD4 T cell subsets in different tissue sites. Ki67 expression by $CD4^+$ naive (red), TCM (blue), and TEM (black) $CD3^+$ T cell subsets in blood, ILN, MLN, and jejunum from Donor 93. Compiled Ki67 data from multiple donors are in Figure S3B.

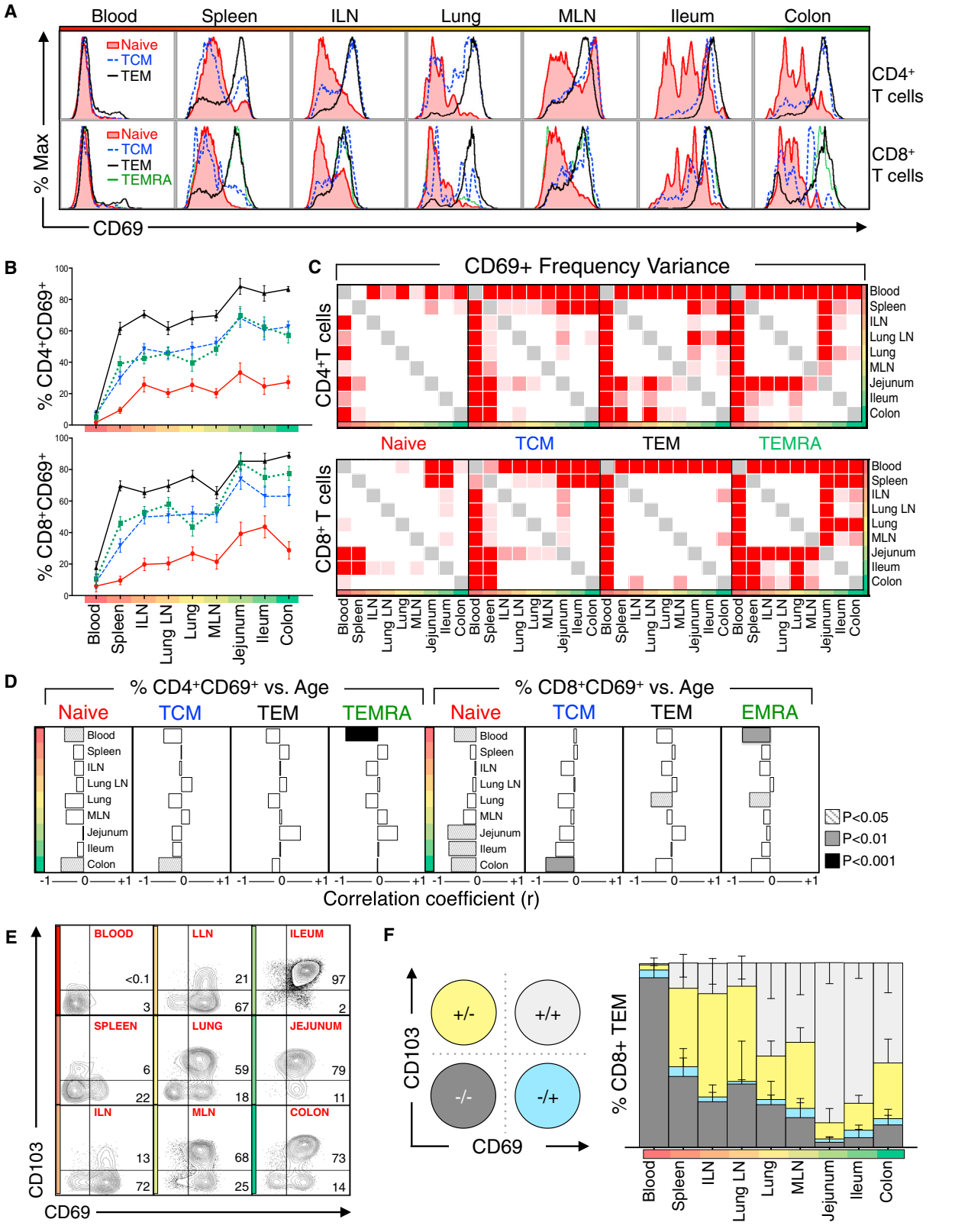


*(legend on next page)*

mucosal sites, shown in a representative flow cytometry plot (Figure 5B) and compiled analysis from 23 donors (Figure 5C). Specifically, the majority of $CD4^+$ TEM (50%–80%) were $CD28^+CD127^+$ in all tissues, with a significant fraction (30%–40%) exhibiting a cytokine-responding $CD28^+CD127^-$ phenotype in lymph nodes, spleen and blood, and low frequency (10%–18%) TCR-responding $CD28^-CD127^+$ TEM in lung and intestines (Figures 5B and 5C and Table S3). By contrast, $CD8^+$ TEM and TEMRA cells were predominantly $CD28^+CD127^-$ in lymphoid tissues and $CD28^-CD127^+$ in mucosal sites, with only low frequency (<20%–40%) $CD28^+CD127^+$ resting populations (Figures 5B and 5C and Table S3). The prevailing $CD28^-$ profile of $CD8^+$ TEM in mucosal sites occurred within the $CD69^+$ TRM fraction (Figures S4A and S4B), suggesting in situ activation of mucosal resident T cells. Additionally, in blood, spleen and lung, significant proportions (23%–26%) of $CD8^+$ TEM and TEMRA cells (and 10% $CD4^+$TEM) were $CD28^-CD127^-$, indicative of circulating activated effector cells (Figure 5C and Table S3).

Variance analyses of population distribution frequencies revealed significant differences in CD28/CD127 coexpression by TEM and TEMRA subsets between blood and lymphoid or blood and mucosal sites, while naive and TCM populations did not vary in CD28/CD127 expression between diverse sites (Figure 5D). $CD4^+$ TEM differed significantly in $CD28^+CD127^+$ and $CD28^+CD127^-$ cell frequency in blood and lymphoid tissue compared to mucosal sites, while $CD8^+$ TEM and TEMRA subsets significantly varied in $CD28^+CD127^+$, $CD28^-CD127^+$, and $CD28^-CD127^-$ population distribution among circulation, lymphoid, and mucosal sites (Figure 5D), indicating compartmentalized maintenance of TEM cells in specific sites. Naive and TCM cells showed no tissue-specific expression differences, indicating that their maintenance is not compartmentalized.

We further quantified the relationship between subset CD28/CD127 coexpression in individual tissues and age through correlation analyses (Figure 6, individual data in Table S5). Significant changes in CD28/CD127 expression occurred primarily in lymphoid tissues, while the CD28/CD127 profile in mucosal sites remained stable over life–another measure of mucosal TEM stability. Notably, both $CD4^+$ and $CD8^+$ TEM cells (and $CD4^+$ TCM cells) increased in $CD28^+CD127^+$ cell frequency with increasing age in lymphoid tissue, particularly in spleen, ILN, and LLN, with a corresponding decrease in $CD28^+CD127^-$ cells (cytokine-responding) for $CD4^+$ T cells, and $CD28^-CD127^+$ or $CD28^-CD127^-$ cells (TCR-stimulated) for $CD8^+$ T cells (Figure 6). This specific population loss and proportional accumulation of resting phenotype $CD28^+CD127^+$ cells suggests homeostatic turnover in the depleted ($CD127^-$ or $CD28^-$) populations. Increased turnover of the $CD4^+CD127^-$ compared to $CD127^+$ subset in lymphoid and mucosal tissues is further supported by increased Ki67 expression (Figure S2B). Together, our analyses of functional markers of homeostasis and residence reveal stability in mucosal sites, dynamic changes in lymphoid tissue, and different patterns of homeostasis between $CD4^+$ and $CD8^+$ TEM.

## TCR Sequencing Reveals Distinct Compartmentalization and Maintenance of $CD4^+$ and $CD8^+$ TEM

We further investigated the mechanisms for the differential homeostasis and maintenance of $CD4^+$ and $CD8^+$ TEM cells by TCR sequencing to quantify the distribution and expansion of individual T cell clones within and between multiple tissues of an individual. Because TCR sequencing identifies all TCR clones within a site and can be affected by sampling errors, we sorted $CD4^+$ and $CD8^+$ TEM cells from spleen and whole lymph nodes (ILN, LLN) to enable analysis of a full complement of tissue-associated T cell subsets. We compared clonal composition of circulating, lymphoid, and mucosal-draining T cells from five donors with ages spanning four decades (Table S6). TCRβ deep sequencing was performed on comparable numbers of TEM cells from each site (Table S6) using the ImmunoSEQ platform (Robins, 2013; Robins et al., 2009). Analysis of nucleotide sequences enabled assessment of clonal overlap and TCR repertoire diversity between tissue sites and T cell subsets (Figure 7 and Extended Experimental Procedures). Of the total clones identified, the proportion shared between sites was different for $CD4^+$ and $CD8^+$ TEM (Figure S5). To eliminate potential sampling issues of rare clones, we assessed the clonal overlap between tissues of the top 500 clones in each site (Figures 7A–7C). Compared to $CD4^+$ TEM, $CD8^+$ TEM had more clones common to all three tissues, consistent in all donors (Figure 7B). Conversely, the majority (>80%) of $CD4^+$TEM clones were unique to each site, while < 50% of $CD8^+$TEM clones were unique, and few TEM clones were shared by only two sites (Figure 7C, left), indicating no specific bias of clonal distribution between sites (Figures 7B and 7C).

The extent of repertoire sharing by each subset was determined by computing the Jaccard index of CD4 and CD8 TEM subsets across all sites for clones greater than 0.05% in

**Figure 4. CD69 Expression Marks T Cell Compartmentalization in Tissue Sites**

(A) Representative flow cytometry histograms showing CD69 expression by $CD4^+$ (top) and $CD8^+$ (bottom) naive (red), TCM (blue), TEM (black), and TEMRA (green) cell subsets from donor #101.

(B) Mean frequency (+- SEM) of $CD69^+$ $CD4^+$ and $CD8^+$ T naive, TCM, TEM, and TEMRA cell subsets among blood, lymphoid, and mucosal tissues. Data shown are compiled from 29 donors (Table S2).

(C) Distribution variance of $CD69^+CD4^+$ (top) and $CD8^+$ (bottom) naive, TCM, TEM, and TEMRA subsets in blood, lymphoid, and mucosal tissues from (B).

(D) Spearman correlation analysis of changes in $CD69^+$ subset tissue distribution with increasing age. Correlation strength and directionality ($r = -1$, left to $r = +1$, right) is shown for each tissue. Correlation significance for each tissue is denoted by shading ($p < 0.05$, striped; $p < 0.01$, gray; $p < 0.001$, black; not significant, white). Individual r- and p values are listed in Table S5).

(E) Representative flow cytometry plots showing CD103/CD69 expression patterns by $CD8^+$ TEM subsets in circulation, lymphoid, and mucosal tissues. Number in upper and lower right quadrants indicate $\%CD69^+CD103^+$ and $\%CD69^+CD103^-$ cells, respectively.

(F) Overall distribution of TEM subpopulations delineated by CD69 and CD103 expression: $CD69^+CD103^+$, light gray; $CD69^+CD103^-$, blue$^-$ $CD69^-$ $CD103^+$, yellow; and $CD69^-$ $CD103^-$, dark gray. Graphs shows mean frequencies (±SEM) of these subsets among $CD8^+$ TEM from nine tissues compiled from 10 donors with each tissue representing 5 or more donors. Individual donors used are indicated in Table S2.

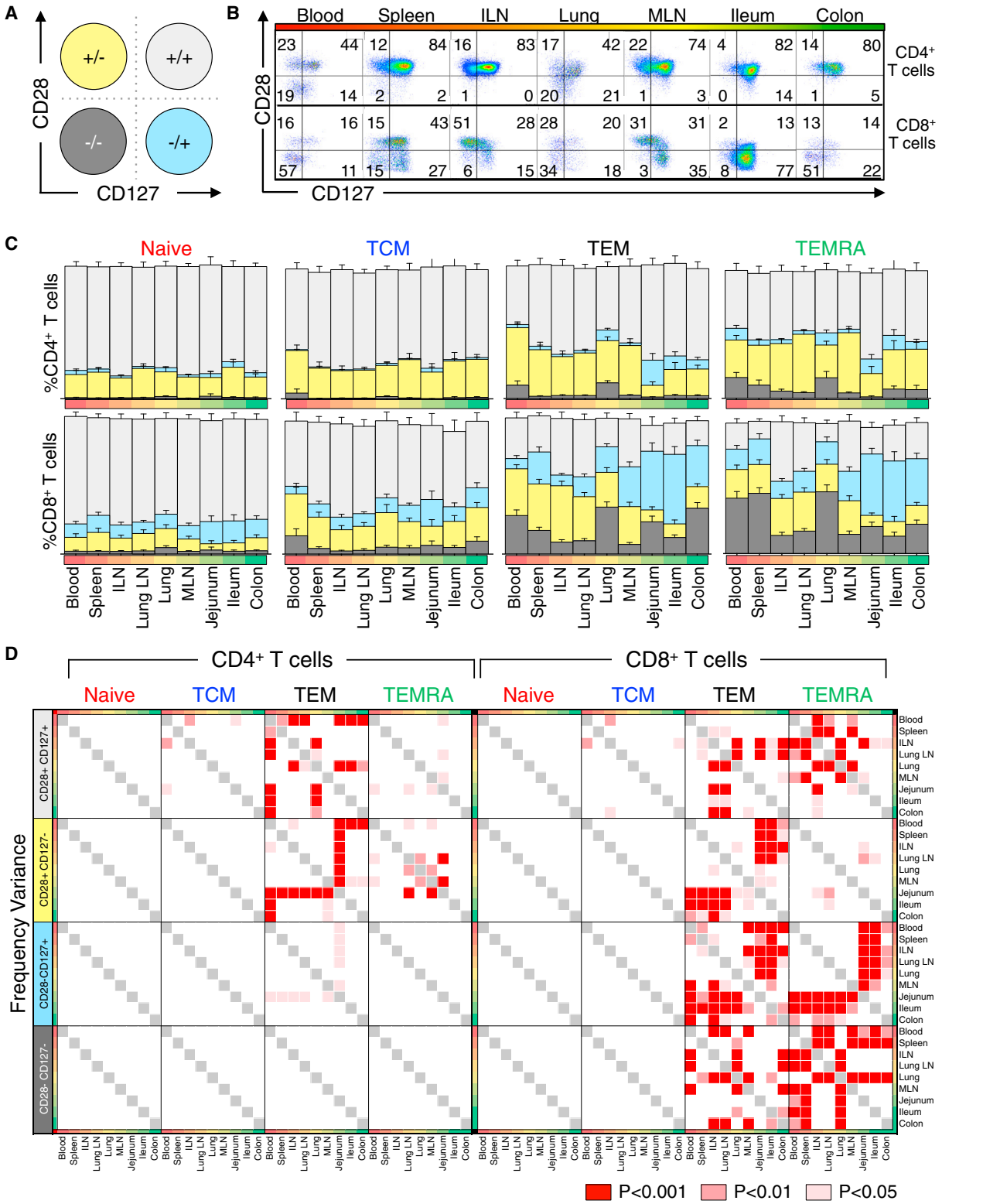


**Figure 5. CD28 and CD127 Expression Reveal Distinct Homeostatic Patterns in Lymphoid and Mucosal Tissues**

Coordinate expression of CD28 and CD127 by $CD4^+$ and $CD8^+$ naive, TCM, TEM, and TEMRA subsets was analyzed.

(A) Diagram showing the 4 subpopulations delineated by CD28/CD127 expression: $CD28^+$ $CD127^+$, light gray; $CD28^-$ $CD127^+$, blue; $CD28^+$ $CD127^-$, yellow; and $CD28^-$ $CD127^-$, dark gray T cells.

*(legend continued on next page)*

frequency, and showed a greater overlap among the CD8$^+$ TEM compared to the CD4$^+$ TEM repertoire (Figures 7D and S6). The Jensen-Shannon (JS) divergence metric quantified differences between repertoire distributions, and revealed that the CD4$^+$ TEM repertoire had increased JS divergence indicating increased TCR diversity compared to CD8$^+$ TEM across all donors and tissues (Figures 7D and S6). Together, this clonal overlap, repertoire sharing, and distribution analysis shows that CD8$^+$ TEM clones are broadly distributed among tissues while CD4$^+$TEM clones remain more compartmentalized.

We next determined whether the increased sharing of CD8$^+$ TEM clones between tissues was due to increased clonal expansion. The degree of clonality was measured for all TCR clones in each tissue site by normalizing the entropy values of each sample to the number of unique TCR sequences, resulting in a value ranging from 0 (most diverse) to 1 (least diverse). CD8$^+$ TEM had higher clonality in all tissue sites in all donors compared to CD4$^+$ TEM (Figure 7E), indicating increased clonal expansion by CD8$^+$ TEM. Between sites, the clonality of spleen CD4$^+$ TEM was significantly greater than that of both ILN and LLN CD4$^+$ TEM, suggesting that circulating CD4$^+$ TEM are more clonally expanded than those in lymph nodes, while CD8$^+$ TEM clonality did not significantly differ between tissues (Figure 7C). Together these results indicate profound and reproducible tissue-specific distinctions between CD4$^+$ and CD8$^+$ TEM clonal diversity. Notably, we found more clonal expansion, less TCR diversity and a broader clonal distribution of CD8$^+$ compared to CD4$^+$ TEM consistent in diverse donors of different ages.

## DISCUSSION

Manipulating human T cell immunity for vaccines and immunotherapies requires a fundamental understanding of the processes driving T cell differentiation and maintenance. Most knowledge of in vivo T cell responses in lymphoid and mucosal tissues derives from studies in mouse models, and translating results to humans has been limited to analysis of peripheral blood. Here, we investigate how human T cells are distributed and maintained in the body using a multidimensional, quantitative analysis of T cell subset differentiation, residence, turnover, and clonal distribution in blood, lymphoid, and mucosal tissues derived from 56 human organ donors spanning over 60 years of life. Our results provide insights into T cell migration, differentiation and maintenance that cannot be extrapolated from studies of T cell subsets in blood. We reveal that the tissue distribution and residence of heterogeneous T cell subsets is contingent on both subset differentiation and tissue-intrinsic factors, and that control of T cell homeostasis depends on tissue localization and CD4$^+$ versus CD8$^+$ lineage. Our elucidation of the human T cell composition in the body and pathways for T cell maintenance over life suggest distinct mechanisms for memory CD4$^+$ and CD8$^+$ T cell differentiation.

Human T cell heterogeneity in blood was initially delineated based on CCR7 expression into two major memory T cell subsets, with CCR7$^+$ TCM cells migrating primarily to lymphoid sites and CCR7$^-$ TEM cells freely circulating in blood, peripheral and nonlymphoid tissue sites (Sallusto et al., 2004; Sallusto et al., 1999). These homing properties for human TCM and TEM cells were mainly extrapolated from ex vivo migration studies and limited analysis of tissue isolates (Campbell et al., 1998; Campbell et al., 2001). When the tissue distribution of these subsets is directly examined among lymphoid and mucosal sites within an individual and compared among many individuals as accomplished here, a far more complex picture emerges. We found that CCR7$^+$ TCM cells comprise a similar proportion of CD4$^+$ T cells in blood, spleen, three different lymph nodes, colon, and ileum, which did not alter with age, and were present in similar proportions to TEM cells in LN. Moreover, loss of CCR7 expression did not reliably indicate exclusion from lymphoid sites: both TEM and TEMRA cells lack CCR7 expression, yet they differed in tissue distribution. TEM represented a significant fraction (>20%–50%) of T cells in lymphoid tissues, while TEMRA cells (exclusively CD8$^+$) were found only in blood, spleen and lung, suggesting a distinct circulatory niche for this subset. Recent studies in mice showing that memory T cell migration is not driven by CCR7 expression (Vander Lugt et al., 2013), and that tissue-homing of CD8$^+$ T cells during allograft rejection occurs independent of chemokine receptor signaling (Walch et al., 2013), further suggest that memory T cell localization is not driven by CCR7 expression. In addition, few CCR7$^+$ TCM cells were found among CD8$^+$ T populations in multiple lymph nodes from over 50 individuals studied, indicating that lymphoid CD8$^+$ T cell memory does not persist as canonical TCM cells.

Additional insights into maintenance and homeostasis of T cell subsets were obtained by examining changes in tissue subset composition within this donor population as a function of age. While it is not possible to directly follow T cell responses in tissues within the same individual over time, the broad and continuous age distribution of our donors, and the consistent tissue T cell subset composition between donors enabled a quantitative analysis of temporal changes in subset composition over decades of life and allowed us to interpolate homeostasis mechanisms and lineage relationships of T cell subsets. We found that lymphoid tissue and blood exhibited the most dynamic changes in subset composition (decreases in naive, increases in TEM subsets) while mucosal sites maintained stable T cell subset frequencies and phenotypes. Ki67 expression showed significant proliferative turnover of TEM and TCM subsets in lymphoid tissue compared to mucosal sites, while naive T cells exhibited minimal turnover, consistent with human studies demonstrating higher turnover of TCM and TEM compared to naive T cells in human blood through $D_2O$ incorporation (De Boer and Perelson, 2013; Macallan et al., 2004) and with in vivo mouse studies in mice showing increased turnover of memory T cells in lymphoid

(B) Representative flow cytometry plots showing pattern of CD28 and CD127 expression by CD4$^+$ (top) and CD8$^+$ (bottom) TEM cells.

(C) Frequency (±SEM) of these functional subsets in (B) within CD4$^+$ (top) and CD8$^+$ (bottom) naive, TCM, TEM, and TEMRA subsets. Individual frequencies from each of 23 donors are in Table S3.

(D) Variance between CD4$^+$ (left) and CD8$^+$ (right) CD127/CD28 subset frequencies within naive, TCM, TEM, and TEMRA subsets was assessed for each tissue by two-way ANOVA and corrected by Holm-Sidak for multiple comparisons. Significant variation among tissues is denoted by colored squares ($p < 0.001$, red; $p < 0.01$, light red; $p < 0.05$, pink). Individual p values for each tissue are listed in Table S4.

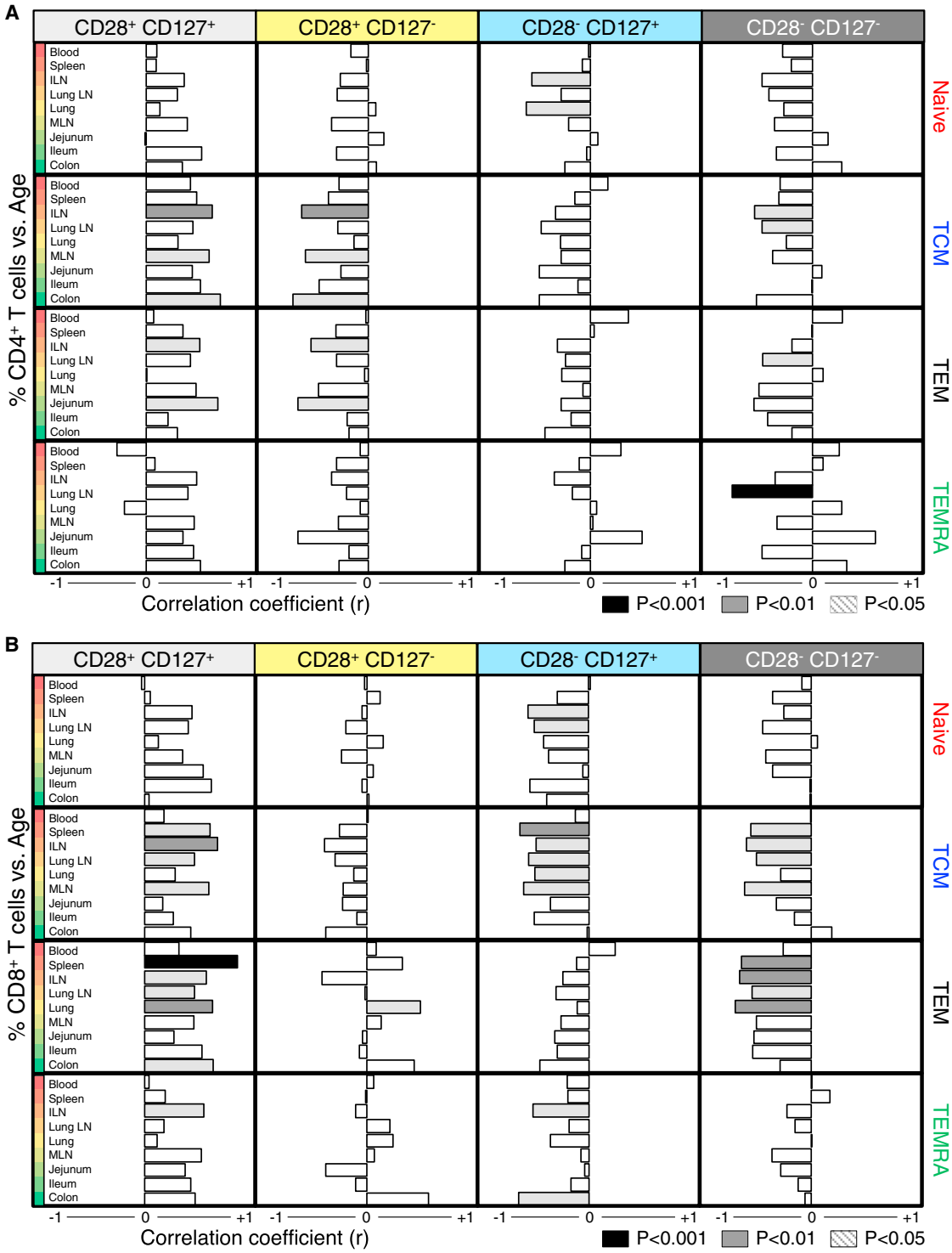


**Figure 6. Temporal Dependence of T Cell Subset Maintenance Is Site Specific**

Correlation between increasing age and frequency of (A) $CD4^+$ and (B) $CD8^+$ naive, TCM, TEM, and TEMRA subsets divided by expression of CD127 and CD28 was determined in each tissue. Correlation degree (bar length) and directionality (left, negative; right, positive) are shown for each population and subset: $CD28^+CD127^+$ (light gray), $CD28^+CD127^-$ (yellow), $CD28^-CD127^+$ (blue), and $CD28^-CD127^-$ (dark gray). Significant correlation is denoted by bar shading ($p < 0.001$ = black, $p < 0.01$ = gray, $p < 0.05$ = light gray). Individual r- and p values for each tissue and subset are shown in Table S5.

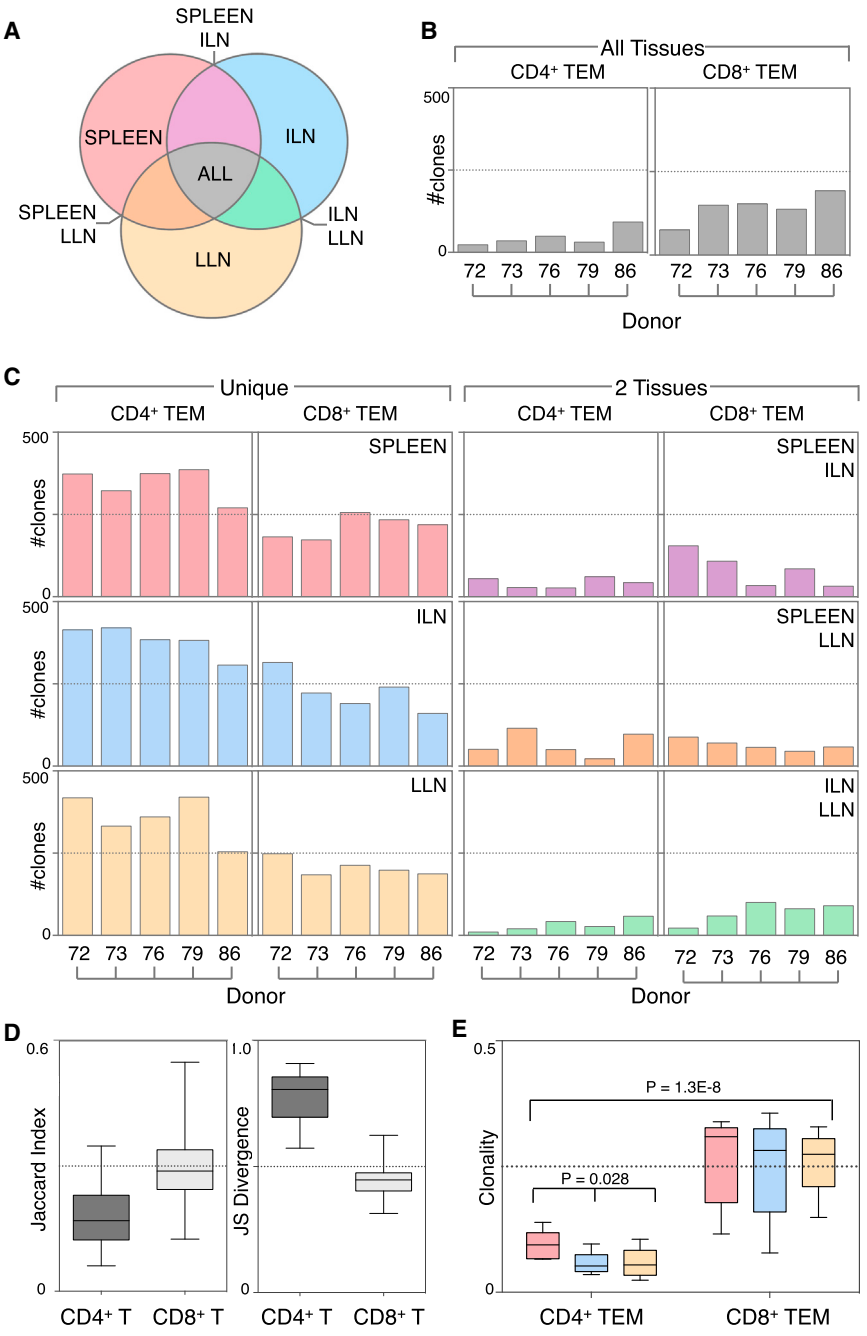


**Figure 7. Differential Clonal Compartmentalization and TCR Diversity between CD4$^+$ and CD8$^+$ TEM Cells**

(A) TCR clonal distribution among and between three tissue sites from five individual donors. Venn diagram schematic showing how TCR clones were grouped according to their tissue distribution indicated by colored shading: TCR sequences unique to spleen (orange-pink), ILN (blue), and LLN (yellow); sequences shared by spleen and LLN but not ILN (orange), spleen and ILN but not LLN (pink), ILN and LLN but not spleen (green); sequences shared by all three tissues (spleen, ILN and LLN) indicated by gray shading.

(B) Clonal TCR sequence overlap of CD4$^+$ and CD8$^+$ TEM in all 3 tissues (spleen, ILN, and LLN) from 5 donors aged 24–55 (Table S1) is shown for the top 500 TCR sequences.

(C) Number of unique TCR clones in each site (left graphs), and clones that were shared specifically between two tissues indicated (right graphs) for CD4$^+$ and CD8$^+$ TEM from five individual donors. TCR sequence data are listed in Table S6.

(D) Left: Jaccard index values of CD4$^+$ (dark gray) and CD8$^+$ (light gray) TEM clones from combined spleen, ILN, and LLN are shown for 5 donors to quantify population similarity. Right: Jensen-Shannon (JS) divergence indices quantify population diversity of CD4$^+$ (dark gray) and CD8$^+$ (light gray) TEM from combined spleen, ILN, and LLN of 5 donors. Individual donor and tissue Jaccard indices and Jensen-Shannon indices are shown in Figure S6A.

(E) Clonality of TCR sequences is shown for CD4$^+$ and CD8$^+$ TEM from spleen (pink), ILN (blue), and LLN (yellow) among 5 donors. Box plots denote 25$^{th}$ to 75$^{th}$ percentile and whiskers indicate minimum and maximum values.

compared to peripheral tissues (Wang et al., 2003). Interestingly, the highest spontaneous turnover of T cell subsets was found in blood, suggesting that the most activated and/or cycling subsets leave the tissues and enter circulation. Though the frequency of TCM cells did not alter with age in blood or any tissue, proliferation of this subset suggests that TCM generation is equally counterbalanced by their turnover. Because loss of naive T cells in lymphoid sites was not associated with turnover, we conclude that loss of naive T cells over time is due to antigen-driven conversion to short-lived effector cells or long-lived memory T cells.

The acquisition of multiple tissues from individual donors enabled a detailed assessment of T cell tissue residence and stability over life not previously possible through studies of blood or isolated tissue biopsies. In particular, we were able to assess the frequency and stability of TRM cells, recently identified as noncirculating, tissue-resident memory T cells marked by CD69 and CD103 expression (Clark, 2010; Farber et al., 2014; Masopust et al., 2006; Mueller et al., 2013; Sathaliyawala et al., 2013). In mouse models, CD69 expression by TRM mediates retention in tissues through degradation of the sphingosine-1-phosphate receptor (S1PR1) (Bankovich et al., 2010; Shiow et al., 2006; Skon et al., 2013). Here, we show that CD69 expression is subset- and tissue-dependent, with human TEM cells in all tissues exhibiting the highest frequency of CD69$^+$ cells while TEM cells in blood and all naive T cells were largely CD69$^-$ (Figure 4). In individuals at all life stages, the highest proportion of CD69$^+$ TEM cells was found

in intestines, suggesting that TRM may be more readily generated and/or stably maintained in mucosal compared to lymphoid sites. The coexpression of CD69 and CD103 by $CD8^+$ TEM in mucosal but not lymphoid tissue further confirms that $CD8^+$ TRM predominate in these sites. Though the precise signals regulating CD69 and CD103 expression by TRM are not known, they likely involve cognate TCR and/or cytokine signals that induce CD69 upregulation (Turner et al., 2014b), and TCR and/or TGF-β signals that trigger CD103 expression (Casey et al., 2012; Wang et al., 2004). Our data further suggest that the signals perceived by TEM in mucosal sites induce molecules controlling long-term retention in situ, and that mucosal TEM/TRM do not readily enter circulation as assessed by an absence of CD69− and CD103− expressing TEM in blood.

Mechanisms for lifelong human T cell maintenance have been difficult to elucidate due to limitations in sampling, although mouse studies demonstrated that homeostatic cytokines such as IL-7 and IL-15 promote memory $CD4^+$ and $CD8^+$ T cell homeostasis (Purton et al., 2007; Surh and Sprent, 2008). Our analysis of CD28/CD127 expression by T cell subsets as functional markers of TCR- or IL-7-mediated signaling, respectively, (Lo et al., 2011; Mazzucchelli and Durum, 2007; Rethi et al., 2005; Warrington et al., 2003) provide evidence for distinct in situ control of human $CD4^+$ and $CD8^+$ T cell maintenance. While naive and TCM persisted as predominant resting ($CD28^+CD127^+$) populations, $CD4^+$ TEM contained significant $CD28^+CD127^-$ (cytokine-responding) populations in all tissues, while $CD8^+$ TEM had predominant $CD28^+CD127^-$ populations in lymphoid sites and $CD28^-CD127^+$ (TCR-responding) populations in mucosal sites. These cytokine-regulated and TCR-stimulated ($CD28^-$) $CD8^+$ and $CD4^+$ TEM cells, respectively, decreased with age specifically in lymphoid tissue, as another indication of homeostatic turnover occurring in lymphoid sites. The $CD28^-CD8^+$ TEM subset in mucosal sites is analogous to $CD28^-$ TEM previously identified in specific inflammatory sites (Martens et al., 1997; Schmidt et al., 1996), and its persistence suggests continuous in situ influences on T cell activation state. It is also notable that blood contained the highest proportion of $CD4^+$ and $CD8^+$ TEM exhibiting an activated ($CD28^-CD127^-$) profile, providing further evidence that the most activated, cycling T cells enter circulation.

We further investigated the different dynamics of $CD4^+$ and $CD8^+$ TEM homeostasis and tissue compartmentalization by T cell clonal analysis using TCRβ deep sequencing. Direct analysis of the individual TCR clones, as defined by a unique nucleotide sequences in the CDR3 region, enabled us to determine whether specific T cell clones represented in one tissue site were also found in others and whether specific clonal expansion occurred in certain subsets and/or tissues. Moreover, our ability to obtain TEM from pooled whole lymph nodes and large segments of spleen reduced sampling bias. Notably, we found increased overlap of TCR clones among $CD8^+$ TEM in mucosal and peripheral-draining lymph nodes and spleen compared to $CD4^+$ TEM, consistent among five donors spanning four decades of life (Figure 7). Clonal analysis of TCR sequences further revealed increased clonality of $CD8^+$ compared to $CD4^+$ TEM, consistent with their increased activation and homeostasis based on CD28/CD127 expression, and the increased overlap of $CD8^+$ compared to $CD4^+$ TEM clones between tissue sites. This increased clonality and TCR-driven maintenance of human memory $CD8^+$ T cells may be a result of ongoing responses to chronic viruses regulated by this subset. $CD4^+$ TEM, however, are less clonally expanded and maintain more clonal diversity and compartmentalization, and therefore may be poised to respond to acute infections.

Current models or T cell differentiation based on studies in mice and human peripheral blood posit either progressive differentiation from naive to memory subsets, and ultimately to terminal effector cells (Restifo and Gattinoni, 2013), or divergent generation of effector and memory subsets as separate lineages (Ahmed et al., 2009; Chang et al., 2007). Our results provide evidence for distinct pathways controlling differentiation and maintenance of human memory $CD4^+$ and $CD8^+$ T cell subsets, with naive $CD4^+$ T cells undergoing progressive differentiation into TCM and TEM cells (Figure S7A), while naive $CD8^+$ T cells divergently generate TEMRA and TEM subsets that migrate through lymphoid tissue and ultimately reside in mucosal sites as resident subsets (Figure S7B). TEM in circulation, lymphoid tissue, and mucosal sites exhibit distinct properties and differentiation states, and TEM which enter tissues are capable of becoming TRM through upregulation of CD69 expression and other retention molecules. Lymphoid TEM and TCM cells undergo the highest degree of turnover, likely replenishing terminal TRM cells lost to attrition (Figure S7).

The findings obtained from our quantitative assessment of T cell immunity in multiple anatomic sites of a diverse population over six decades of human life, have broad implications for improving immune monitoring, vaccines and immunotherapies. Our study makes important advances in demonstrating how peripheral blood T cells relate to in situ tissue responses, with peripheral blood containing more activated and cycling cells compared to tissues. We also demonstrate that CD8 T cells have distinct differentiation fates and maintenance mechanisms compared to CD4 T cells, which is of great relevance for designing vaccines and monitoring their efficacy. Finally, our analyses provide a dynamic map of T cell composition in healthy tissues over life, and establish a standard from which to define immune health and homeostasis and better understand tissue-specific and immune-associated pathologies.

## EXPERIMENTAL PROCEDURES

### Acquisition of Human Tissues

Human tissues were obtained from deceased organ donors at the time of organ acquisition for clinical transplantation through an approved research protocol and MTA with the NYODN. All donors were free of chronic disease and cancer, were Hepatitis B-, C-, and HIV-negative. Tissues were collected after the donor organs were flushed with cold preservation solution and clinical procurement process was completed. The study does not qualify as "human subjects" research, as confirmed by the Columbia University IRB as tissue samples were obtained from brain-dead (deceased) individuals.

### Lymphocyte Isolation from Human Lymphoid and Nonlymphoid Tissues

Tissue samples were maintained in cold saline and brought to the laboratory within 2–4 hr of organ procurement. Samples were rapidly processed using enzymatic and mechanical digestion resulting in high yields of live

lymphocytes, as described (Sathaliyawala et al., 2013) with additional optimizations detailed in Extended Experimental Procedures.

### Flow Cytometry Analysis

The following flurochrome-conjugated antibodies were used: anti-human CD3 (Brilliant Violet 650, OKT3, BioLegend, San Diego, CA), CD4 (PeCy7, SK3, BioLegend), CD8 (APC-Cy7, SK1, BD Biosciences, San Jose, CA), CD19 (PE Texas Red, SJ25-C1, Life Technologies, Carlsbad, CA), CD28 (PE, CD28.2, eBioscience, San Diego, CA), CD45RA (Brilliant Violet 605, HI100, BioLegend), CD45RO (PerCpFl710, UCHL1, eBioscience), CD69 (Brilliant Violet 421, FN50, BioLegend), CD103 (Alexa Fluor 647, Ber-Act8, Biolegend), CD127 (Brilliant Violet 711, BioLegend), and CCR7 (Alexa Fluor 488, TG8, BioLegend). Stained cells were acquired on a 6-laser LSRII analytical flow cytometry (BD Biosciences, San Jose, CA). Control samples included unstained and single fluorochrome-stained compensation beads (OneComp ebeads, eBioscience) for accurate compensation and subsequent data analysis. Flow cytometry data were analyzed using FlowJo software (Treestar, Ashland, OR).

### Cell Proliferation Analysis

To monitor cell proliferation, cells were stained for surface markers followed by fixation and permeabilization with in specific buffers (eBioscience), and stained with Ki67 (PE, B56, BD Biosciences) and analyzed by flow cytometry.

### Statistical Analysis and Data Visualization

Descriptive statistics (percent means, standard deviations, counts) were calculated for each T cell subset and tissue in Microsoft Excel. Frequency variance was determined for each subset and tissue by Holm-Sidak post hoc multiple comparison following two-way ANOVA to exclude subset-dependent effects in GraphPad PRISM (Graphpad software, La Jolla, CA). Frequency comparison p values for each tissue versus each remaining tissue were graphed using Microsoft Excel. Correlation analysis of subset distribution versus age was calculated in GraphPad PRISM by nonparametric Spearman correlation for non-Gaussian distributions. Resulting two-tailed p values and r values were graphed in Microsoft Excel and using GraphPad Prism.

### T Cell Receptor Sequencing

TEM-phenotype ($CD45RA^{-}CCR7^{-}$) $CD4^{+}$ and $CD8^{+}$ T cells were sorted from 2–3 whole lymph nodes for ILN and LLN and large pieces (7 $cm^2$) of human spleen obtained from five individual donors (donors 72, 73, 76, 79, 86; Tables S1 and S2) using a BD-influx cell sorter (BD Biosciences). Purified populations were sent to Adaptive Biotechnologies (Seattle, WA) for TCRβ deep sequencing using the ImmunoSEQ platform (Robins et al., 2009). Cell number and productive reads for each population from each donor are presented in Table S6. Analysis of nucleotide sequences for repertoire overlap, TCR diversity and clonality were calculated using R-based approaches as detailed in the extended methods in supplementary information.

## SUPPLEMENTAL INFORMATION

Supplemental Information includes Extended Experimental Procedures, seven figures, and six tables and can be found with this article online at http://dx.doi.org/10.1016/j.cell.2014.10.026.

## AUTHOR CONTRIBUTIONS

J.J.T. and N.Y. contributed equally to this work. J.J.T. processed donor tissues, performed flow cytometry, collected the data, and wrote the paper; N.Y. performed statistical analyses, visualized the data, created models and wrote the paper. Y.O., T.S., and M.K. performed surgical acquisition of donor tissues and helped with tissue processing. H.L. coordinated tissue donation and acquisition. B.G. and Y.S. analyzed the TCR sequencing data and calculated the different parameters for diversity, clonality and normalized entropy. D.L.F. planned experiments, coordinated tissue acquisition and data acquisition/analysis, analyzed data, and wrote the paper.

## ACKNOWLEDGMENTS

This work was supported by NIH P01AI06697 awarded to D.L.F. J.J.T is supported by NIH F31AG047003 and a BD Bioscience Immunology Research Grant. These studies were performed in the CCTI Flow Cytometry Core funded in part through an S10 Shared Instrumentation Grant, 1S10RR027050. We wish to gratefully acknowledge the generosity of the donor families and the outstanding efforts of the NYODN transplant coordinators and staff for making this study possible. We also wish to thank Dr. Claire Gordon and Mr. Sam Mickel for assistance with tissue processing, and Drs. Uri Hershberg and Claire Gordon for critical reading of this manuscript.

Received: May 12, 2014
Revised: August 8, 2014
Accepted: September 24, 2014
Published: November 6, 2014

## REFERENCES

Ahmed, R., Bevan, M.J., Reiner, S.L., and Fearon, D.T. (2009). The precursors of memory: models and controversies. Nat. Rev. Immunol. *9*, 662–668.

Bankovich, A.J., Shiow, L.R., and Cyster, J.G. (2010). CD69 suppresses sphingosine 1-phosophate receptor-1 (S1P1) function through interaction with membrane helix 4. J. Biol. Chem. *285*, 22328–22337.

Campbell, J.J., Bowman, E.P., Murphy, K., Youngman, K.R., Siani, M.A., Thompson, D.A., Wu, L., Zlotnik, A., and Butcher, E.C. (1998). 6-C-kine (SLC), a lymphocyte adhesion-triggering chemokine expressed by high endothelium, is an agonist for the MIP-3beta receptor CCR7. J. Cell Biol. *141*, 1053–1059.

Campbell, J.J., Murphy, K.E., Kunkel, E.J., Brightling, C.E., Soler, D., Shen, Z., Boisvert, J., Greenberg, H.B., Vierra, M.A., Goodman, S.B., et al. (2001). CCR7 expression and memory T cell diversity in humans. J. Immunol. *166*, 877–884.

Casey, K.A., Fraser, K.A., Schenkel, J.M., Moran, A., Abt, M.C., Beura, L.K., Lucas, P.J., Artis, D., Wherry, E.J., Hogquist, K., et al. (2012). Antigen-independent differentiation and maintenance of effector-like resident memory T cells in tissues. J. Immunol. *188*, 4866–4875.

Chang, J.T., Palanivel, V.R., Kinjyo, I., Schambach, F., Intlekofer, A.M., Banerjee, A., Longworth, S.A., Vinup, K.E., Mrass, P., Oliaro, J., et al. (2007). Asymmetric T lymphocyte division in the initiation of adaptive immune responses. Science *315*, 1687–1691.

Clark, R.A. (2010). Skin-resident T cells: the ups and downs of on site immunity. J. Invest. Dermatol. *130*, 362–370.

Clark, R.A., Chong, B., Mirchandani, N., Brinster, N.K., Yamanaka, K., Dowgiert, R.K., and Kupper, T.S. (2006). The vast majority of CLA+ T cells are resident in normal skin. J. Immunol. *176*, 4431–4439.

De Boer, R.J., and Perelson, A.S. (2013). Quantifying T lymphocyte turnover. J. Theor. Biol. *327*, 45–87.

Farber, D.L., Yudanin, N.A., and Restifo, N.P. (2014). Human memory T cells: generation, compartmentalization and homeostasis. Nat. Rev. Immunol. *14*, 24–35.

Ganusov, V.V., and De Boer, R.J. (2007). Do most lymphocytes in humans really reside in the gut? Trends Immunol. *28*, 514–518.

Kiazyk, S.A., and Fowke, K.R. (2008). Loss of CD127 expression links immune activation and CD4(+) T cell loss in HIV infection. Trends Microbiol. *16*, 567–573.

Lo, D.J., Weaver, T.A., Stempora, L., Mehta, A.K., Ford, M.L., Larsen, C.P., and Kirk, A.D. (2011). Selective targeting of human alloresponsive CD8+ effector memory T cells based on CD2 expression. Am. J. Transplant. *11*, 22–33.

Macallan, D.C., Wallace, D., Zhang, Y., De Lara, C., Worth, A.T., Ghattas, H., Griffin, G.E., Beverley, P.C., and Tough, D.F. (2004). Rapid turnover of effector-memory CD4(+) T cells in healthy humans. J. Exp. Med. *200*, 255–260.

Martens, P.B., Goronzy, J.J., Schaid, D., and Weyand, C.M. (1997). Expansion of unusual CD4+ T cells in severe rheumatoid arthritis. Arthritis Rheum. *40*, 1106–1114.

Masopust, D., Vezys, V., Wherry, E.J., Barber, D.L., and Ahmed, R. (2006). Cutting edge: gut microenvironment promotes differentiation of a unique memory CD8 T cell population. J. Immunol. *176*, 2079–2083.

Mazzucchelli, R., and Durum, S.K. (2007). Interleukin-7 receptor expression: intelligent design. Nat. Rev. Immunol. *7*, 144–154.

Mueller, S.N., Gebhardt, T., Carbone, F.R., and Heath, W.R. (2013). Memory T cell subsets, migration patterns, and tissue residence. Annu. Rev. Immunol. *31*, 137–161.

Purton, J.F., Tan, J.T., Rubinstein, M.P., Kim, D.M., Sprent, J., and Surh, C.D. (2007). Antiviral CD4+ memory T cells are IL-15 dependent. J. Exp. Med. *204*, 951–961.

Purwar, R., Campbell, J., Murphy, G., Richards, W.G., Clark, R.A., and Kupper, T.S. (2011). Resident memory T cells (T(RM)) are abundant in human lung: diversity, function, and antigen specificity. PLoS ONE *6*, e16245.

Restifo, N.P., and Gattinoni, L. (2013). Lineage relationship of effector and memory T cells. Curr. Opin. Immunol. *25*, 556–563.

Rethi, B., Fluur, C., Atlas, A., Krzyzowska, M., Mowafi, F., Grützmeier, S., De Milito, A., Bellocco, R., Falk, K.I., Rajnavölgyi, E., and Chiodi, F. (2005). Loss of IL-7Ralpha is associated with CD4 T-cell depletion, high interleukin-7 levels and CD28 down-regulation in HIV infected patients. AIDS *19*, 2077–2086.

Robins, H. (2013). Immunosequencing: applications of immune repertoire deep sequencing. Curr. Opin. Immunol. *25*, 646–652.

Robins, H.S., Campregher, P.V., Srivastava, S.K., Wacher, A., Turtle, C.J., Kahsai, O., Riddell, S.R., Warren, E.H., and Carlson, C.S. (2009). Comprehensive assessment of T-cell receptor beta-chain diversity in alphabeta T cells. Blood *114*, 4099–4107.

Sallusto, F., Lenig, D., Förster, R., Lipp, M., and Lanzavecchia, A. (1999). Two subsets of memory T lymphocytes with distinct homing potentials and effector functions. Nature *401*, 708–712.

Sallusto, F., Geginat, J., and Lanzavecchia, A. (2004). Central memory and effector memory T cell subsets: function, generation, and maintenance. Annu. Rev. Immunol. *22*, 745–763.

Sathaliyawala, T., Kubota, M., Yudanin, N., Turner, D., Camp, P., Thome, J.J., Bickham, K.L., Lerner, H., Goldstein, M., Sykes, M., et al. (2013). Distribution and compartmentalization of human circulating and tissue-resident memory T cell subsets. Immunity *38*, 187–197.

Saule, P., Trauet, J., Dutriez, V., Lekeux, V., Dessaint, J.P., and Labalette, M. (2006). Accumulation of memory T cells from childhood to old age: central and effector memory cells in CD4(+) versus effector memory and terminally differentiated memory cells in CD8(+) compartment. Mech. Ageing Dev. *127*, 274–281.

Schmidt, D., Goronzy, J.J., and Weyand, C.M. (1996). CD4+ CD7- CD28- T cells are expanded in rheumatoid arthritis and are characterized by autoreactivity. J. Clin. Invest. *97*, 2027–2037.

Schön, M.P., Arya, A., Murphy, E.A., Adams, C.M., Strauch, U.G., Agace, W.W., Marsal, J., Donohue, J.P., Her, H., Beier, D.R., et al. (1999). Mucosal T lymphocyte numbers are selectively reduced in integrin alpha E (CD103)-deficient mice. J. Immunol. *162*, 6641–6649.

Shiow, L.R., Rosen, D.B., Brdicková, N., Xu, Y., An, J., Lanier, L.L., Cyster, J.G., and Matloubian, M. (2006). CD69 acts downstream of interferon-alpha/beta to inhibit S1P1 and lymphocyte egress from lymphoid organs. Nature *440*, 540–544.

Skon, C.N., Lee, J.Y., Anderson, K.G., Masopust, D., Hogquist, K.A., and Jameson, S.C. (2013). Transcriptional downregulation of S1pr1 is required for the establishment of resident memory CD8+ T cells. Nat. Immunol. *14*, 1285–1293.

Strauch, U.G., Mueller, R.C., Li, X.Y., Cernadas, M., Higgins, J.M., Binion, D.G., and Parker, C.M. (2001). Integrin alpha E(CD103)beta 7 mediates adhesion to intestinal microvascular endothelial cell lines via an E-cadherin-independent interaction. J. Immunol. *166*, 3506–3514.

Surh, C.D., and Sprent, J. (2008). Homeostasis of naive and memory T cells. Immunity *29*, 848–862.

Turner, D.L., Bickham, K.L., Thome, J.J., Kim, C.Y., D'Ovidio, F., Wherry, E.J., and Farber, D.L. (2014a). Lung niches for the generation and maintenance of tissue-resident memory T cells. Mucosal Immunol. *7*, 501–510.

Turner, D.L., Gordon, C.L., and Farber, D.L. (2014b). Tissue-resident T cells, in situ immunity and transplantation. Immunol. Rev. *258*, 150–166.

Vallejo, A.N., Brandes, J.C., Weyand, C.M., and Goronzy, J.J. (1999). Modulation of CD28 expression: distinct regulatory pathways during activation and replicative senescence. J. Immunol. *162*, 6572–6579.

Vander Lugt, B., Tubo, N.J., Nizza, S.T., Boes, M., Malissen, B., Fuhlbrigge, R.C., Kupper, T.S., and Campbell, J.J. (2013). CCR7 plays no appreciable role in trafficking of central memory CD4 T cells to lymph nodes. J. Immunol. *191*, 3119–3127.

Walch, J.M., Zeng, Q., Li, Q., Oberbarnscheidt, M.H., Hoffman, R.A., Williams, A.L., Rothstein, D.M., Shlomchik, W.D., Kim, J.V., Camirand, G., and Lakkis, F.G. (2013). Cognate antigen directs CD8+ T cell migration to vascularized transplants. J. Clin. Invest. *123*, 2663–2671.

Wang, X.Z., Stepp, S.E., Brehm, M.A., Chen, H.D., Selin, L.K., and Welsh, R.M. (2003). Virus-specific CD8 T cells in peripheral tissues are more resistant to apoptosis than those in lymphoid organs. Immunity *18*, 631–642.

Wang, D., Yuan, R., Feng, Y., El-Asady, R., Farber, D.L., Gress, R.E., Lucas, P.J., and Hadley, G.A. (2004). Regulation of CD103 expression by CD8+ T cells responding to renal allografts. J. Immunol. *172*, 214–221.

Warrington, K.J., Vallejo, A.N., Weyand, C.M., and Goronzy, J.J. (2003). CD28 loss in senescent CD4+ T cells: reversal by interleukin-12 stimulation. Blood *101*, 3543–3549.